Maneuvering Target Tracking Using Retrospective-Cost Input Estimation

LIANG HAN, Student Member, IEEE
ZHANG REN
Beihang University
Beijing, P. R. China

DENNIS S. BERNSTEIN, Fellow, IEEE
University of Michigan
Ann Arbor MI, USA

This paper uses a Kalman filter with retrospective cost–based input estimation (KF/RCIE) to track maneuvering targets with unknown acceleration. Unlike conventional tracking methods that model the acceleration as a random process, KF/RCIE views the unknown acceleration as a deterministic unknown signal. Retrospective cost optimization is then used to estimate the unknown acceleration. Numerical examples and laboratory experiments illustrate the effectiveness of this approach with comparison to conventional tracking methods.

Manuscript received July 21, 2015; revised December 16, 2015, April 13, 2016; released for publication May 20, 2016.

DOI. No. 10.1109/TAES.2016.150186.

Refereeing of this contribution was handled by F. Govaers.

This work was supported by the National Natural Science Foundation of China under Grant 61333011.

Authors' addresses: L. Han, Z. Ren, Beihang University, School of Automation Science and Electrical Engineering, Xueyuan Road No. 37, Haidian District, Beijing 100191, P. R. China; D. S. Bernstein, Department of Aerospace Engineering, 3020 FXB Building, 1320 Beal Street, University of Michigan, Ann Arbor, MI 48109-2140. Corresponding author is L. Han, E-mail: (lianghan@buaa.edu.cn).

I. INTRODUCTION

Input and state estimation techniques for tracking maneuvering targets can be classified into two categories [1]. The first is to treat the acceleration input as the state of a random process, such as white noise, a Markov process, or a semi-Markov jump process. The constant-acceleration (CA) model and constant-turn model [2] are the basic maneuvering models. A classic example is the Singer tracking model [3–5], which models the target acceleration as a first-order, zero-mean Markov process. The current statistical model [6] assumes that the acceleration is unknown but that the change in acceleration is limited. The jerk-tracking model [7, 8] assumes that the acceleration derivative is an independent process of higher order. The above models work well for estimating the acceleration input when the acceleration is nonzero but are inefficient when the velocity is constant. In order to improve the estimation accuracy, the interacting multiple model (IMM) approach [9–13] combines multiple tracking models under switching. This approach requires a sufficient number of models to adequately describe the target maneuvering dynamics. However, the computational complexity increases with the number of models. Extensions of IMM are introduced in [14]. The variable-structure multiple-model (VSMM) method is presented in [15]. In contrast to IMM, which contains a fixed model set, VSMM adjusts the model set in real time to reduce the computational complexity.

An alternative approach is to treat the acceleration as an unknown deterministic signal that can be estimated. In [16], the Kalman filter is combined with a least-squares input estimator to estimate the state and acceleration input. The approach of [17] extends this method and presents a multiple-model–based recursive algorithm. An improved estimation method that incorporates a maneuver detection window is given in [18]. This method does not require multiple models and has lower computational cost. In [19], a Kalman-filter–based input estimation method is developed. The acceleration component is added to the state vector, and the Kalman filter is used to optimize the augmented state vector. However, this method is efficient only for constant acceleration. The technique given in [20] provides a linear minimum-variance unbiased estimate of the state and unknown input. In [21], a recursive three-step filter is presented where the estimates of the state and input are interconnected. However, global optimality of this filter cannot be guaranteed. An estimator that allows recovery of both the state and unknown input after a delay is presented in [22]. This approach can be used for left-invertible systems without invariant zeros. The technique in [23] estimates the state with input reconstruction based on a reduced-order delayed-state observer. In [24], an unknown input observer is developed for linear time-invariant systems. Compared with previous estimators, this estimator can be used for nonminimum-phase systems.

In the present paper, we consider input estimation using a retrospective cost technique. Retrospective cost

optimization was developed for adaptive control in [25, 26] and applied to input and state estimation in [27]. This method optimizes a retrospective cost function to drive the output of the feedback system (that is, the output error) to zero and estimates the input along with the states of the system. This technique is used with the Kalman filter in [28] to estimate the state of a nonminimum-phase system with uncertain harmonic inputs and in [29] to estimate the acceleration of an aircraft.

In this paper, we combine retrospective-cost–input estimation with the Kalman filter (KF/RCIE) to estimate the acceleration of a maneuvering target. RCIE optimizes the retrospective performance to estimate the acceleration, which is then used by the Kalman filter along with measurements to estimate the state. KF/RCIE is different from other estimation methods in several ways. In particular, the traditional Kalman filter treats the unknown acceleration input as a random process. Conventional input and state estimators require knowledge of the distribution of the input in [30–35]. However, KF/RCIE requires no prior information about the input.

We investigate the performance of KF/RCIE by simulation examples and laboratory experiments. The tracking system includes an Optitrack camera system and a rate table. The Optitrack camera system captures the 3D position of a rigid body by using markers and cameras. The paper is organized as follows. In Section II, KF/RCIE is formulated, and RCIE is developed in Section III. In Section IV, the maneuvering target tracking problem is addressed. KF/RCIE is used for maneuvering target tracking with noise measurements, and rate-table target tracking experiments are considered in Section V. Finally, conclusions are drawn in Section VI.

II. PROBLEM FORMULATION

Consider the linear time-invariant system

$$x(k) = Ax(k-1) + Bu(k-1) + w(k-1), \tag{1}$$

$$y(k) = Cx(k) + v(k), \tag{2}$$

where $x(k) \in \mathbb{R}^{l_x}$ is the state, $u(k) \in \mathbb{R}^{l_u}$ is the input, $w(k) \in \mathbb{R}^{l_w}$ is the process noise with covariance $Q(k) \in \mathbb{R}^{l_x \times l_x}$, $y(k) \in \mathbb{R}^{l_y}$ is the measured output, and $v(k) \in \mathbb{R}^{l_v}$ is the measurement noise with covariance $R(k) \in \mathbb{R}^{l_y \times l_y}$. The matrices $A \in \mathbb{R}^{l_x \times l_x}$, $B \in \mathbb{R}^{l_x \times l_u}$, and $C \in \mathbb{R}^{l_y \times l_x}$ are assumed to be known.

The Kalman filter consists of two steps. The forecast step is given by

$$x_{\mathrm{f}}(k) = Ax_{\mathrm{da}}(k-1) + Bu(k-1), \tag{3}$$

$$P_{\mathrm{f}}(k) = AP_{\mathrm{da}}(k-1)A^{\mathrm{T}} + Q(k-1), \tag{4}$$

where $x_{\mathrm{f}}(k) \in \mathbb{R}^{l_x}$ is the forecast state, $x_{\mathrm{da}}(k) \in \mathbb{R}^{l_x}$ is the data assimilation state, $P_{\mathrm{f}}(k) \in \mathbb{R}^{l_x \times l_x}$ is the forecast error covariance, and $P_{\mathrm{da}}(k) \in \mathbb{R}^{l_x \times l_x}$ is the data assimilation error covariance. The data assimilation step is given by

$$K_{\mathrm{da}}(k) = P_{\mathrm{f}}(k)C^{\mathrm{T}}S_{\mathrm{da}}^{-1}(k), \tag{5}$$

$$P_{\mathrm{da}}(k) = P_{\mathrm{f}}(k) - P_{\mathrm{f}}(k)C^{\mathrm{T}}S_{\mathrm{da}}^{-1}(k)CP_{\mathrm{f}}(k), \tag{6}$$

$$x_{\mathrm{da}}(k) = x_{\mathrm{f}}(k) + K_{\mathrm{da}}(k)\left[y(k) - Cx_{\mathrm{f}}(k)\right], \tag{7}$$

where $K_{\mathrm{da}}(k) \in \mathbb{R}^{l_x \times l_y}$ is the state estimator gain and $S_{\mathrm{da}}(k) \triangleq CP_{\mathrm{f}}(k)C^{\mathrm{T}} + R(k)$.

If the input $u(k)$ is unknown, (3) cannot be implemented. In this case, the effect of $u(k)$ may be included in the process noise $w(k)$ by a suitable choice of $Q(k)$. Alternatively, it may be more desirable to estimate the unknown input and replace $u(k)$ in (3) by an estimated input $\hat{u}(k)$. In this case, (3) is replaced by

$$x_{\mathrm{f}}(k) = Ax_{\mathrm{da}}(k-1) + B\hat{u}(k-1). \tag{8}$$

In order to estimate $u(k)$, we construct an adaptive input estimator of the form

$$\hat{x}(k) = A\hat{x}(k-1) + B\hat{u}(k-1), \tag{9}$$

$$\hat{y}(k) = C\hat{x}(k), \tag{10}$$

$$z(k) = y(k) - \hat{y}(k), \tag{11}$$

where $\hat{x}(k) \in \mathbb{R}^{l_x}$ is the estimated state, $\hat{y}(k) \in \mathbb{R}^{l_y}$ is the estimated output, and $z(k) \in \mathbb{R}^{l_z}$ is the output error. The estimated input $\hat{u}(k)$ is the output of the input estimation subsystem of order n_e given by

$$\hat{u}(k) = \sum_{i=1}^{n_{\mathrm{e}}} P_i(k)\hat{u}(k-i) + \sum_{i=1}^{n_{\mathrm{e}}} Q_i(k)z(k-i), \tag{12}$$

where $P_i(k) \in \mathbb{R}^{l_u \times l_u}$ and $Q_i(k) \in \mathbb{R}^{l_u \times l_z}$ are the input estimator coefficient matrices. We rewrite (12) as

$$\hat{u}(k) = \Phi(k)\theta(k), \tag{13}$$

where the regressor matrix $\Phi(k)$ is defined by

$$\Phi(k) \triangleq \begin{bmatrix} \hat{u}(k-1) \\ \vdots \\ \hat{u}(k-n_{\mathrm{e}}) \\ z(k-1) \\ \vdots \\ z(k-n_{\mathrm{e}}) \end{bmatrix}^{\mathrm{T}} \otimes I_{l_u} \in \mathbb{R}^{l_u \times l_\theta} \tag{14}$$

and the estimator coefficient vector $\theta(k)$ is defined by

$$\theta(k) \triangleq \mathrm{vec}\left[P_1(k)\ \cdots\ P_{n_{\mathrm{e}}}(k)\ Q_1(k)\ \cdots\ Q_{n_{\mathrm{e}}}(k)\right] \in \mathbb{R}^{l_\theta}, \tag{15}$$

where $l_\theta \triangleq l_u^2 n_{\mathrm{e}} + l_u l_z n_{\mathrm{e}}$, $\otimes$ is the Kronecker product, and vec is the column-stacking operator. Fig. 1 shows the structure of KF/RCIE.

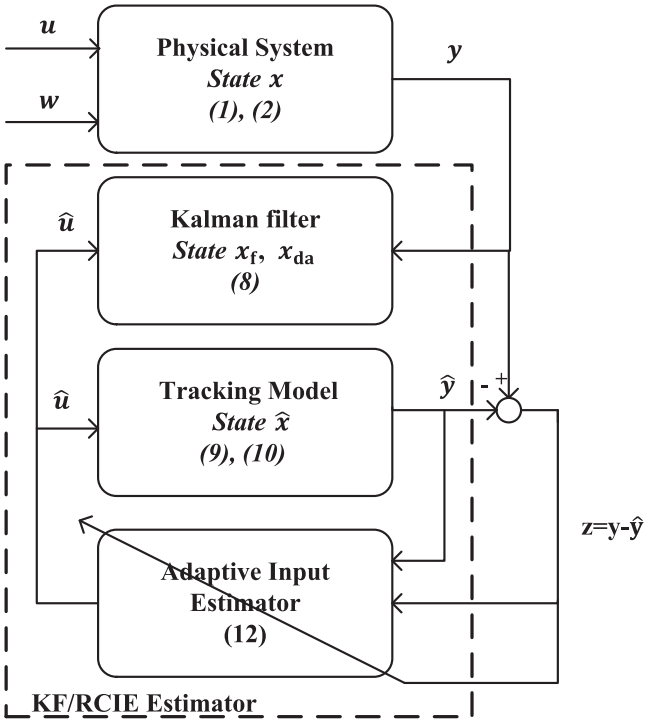

Fig. 1. KF/RCIE estimator.

III. INPUT ESTIMATION USING RETROSPECTIVE COST

A. Retrospective Performance

We define the retrospective performance variable as

$$\hat{z}(k) \triangleq z(k) + \Phi_{\mathrm{f}}(k)\hat{\theta} - u_{\mathrm{f}}(k), \tag{16}$$

where $\hat{\theta} \in \mathbb{R}^{l_\theta}$ is determined by optimization below and $\Phi_{\mathrm{f}}(k) \in \mathbb{R}^{l_z \times l_\theta}$ and $u_{\mathrm{f}}(k) \in \mathbb{R}^{l_z}$ are filtered versions of $\Phi(k)$ and $u(k)$, respectively, defined by

$$\Phi_{\mathrm{f}}(k) \triangleq G_{\mathrm{f}_u}(\mathbf{z})\Phi(k), \tag{17}$$

$$u_{\mathrm{f}}(k) \triangleq G_{\mathrm{f}_u}(\mathbf{z})u(k), \tag{18}$$

where $\mathbf{z}$ represents the forward shift operator. The filter $G_{\mathrm{f}_u}(\mathbf{z}) \in \mathbb{R}^{l_z \times l_u}$ has the form

$$G_{\mathrm{f}_u}(\mathbf{z}) \triangleq D_u^{-1}(\mathbf{z})N_u(\mathbf{z}), \tag{19}$$

where $N_u(\mathbf{z}) \triangleq M_1\mathbf{z}^{n_{\mathrm{f}}-1} + M_2\mathbf{z}^{n_{\mathrm{f}}-2} + \cdots + M_{n_{\mathrm{f}}}$ and $D_u(\mathbf{z}) \triangleq I_{l_z}\mathbf{z}^{n_{\mathrm{f}}} + N_1\mathbf{z}^{n_{\mathrm{f}}-1} + N_2\mathbf{z}^{n_{\mathrm{f}}-2} + \cdots + N_{n_{\mathrm{f}}}$ with $M_i \in \mathbb{R}^{l_z \times l_u}$ and $N_i \in \mathbb{R}^{l_z \times l_z}$ and $n_{\mathrm{f}} \geq 1$ is the order of G_{f_u}.

B. Markov Parameters

The filter G_{f_u} is based on the Markov parameters of the input-to-performance transfer function $G_{zu}(\mathbf{z}) = C(\mathbf{z}I - A)^{-1}B$. For all complex numbers $\mathbf{z}$ whose absolute value is greater than the spectral radius of A, it follows that

$$G_{zu}(\mathbf{z}) = \sum_{i=0}^{\infty} \frac{H_i}{\mathbf{z}^i}, \tag{20}$$

where, for all $i \geq 1$, the ith Markov parameter of G_{zu} is defined by

$$H_i \triangleq CA^{i-1}B. \tag{21}$$

In this paper, G_{f_u} is chosen to be the Markov-parameter–based finite-impulse-response filter of order n_{f} given by

$$G_{\mathrm{f}_u}(\mathbf{z}) = \sum_{i=0}^{n_{\mathrm{f}}} \frac{H_i}{\mathbf{z}^i}. \tag{22}$$

C. Retrospective Cost Function

Using the retrospective performance variable $\hat{z}(k)$, we define the retrospective cost

$$J(k, \hat{\theta}) \triangleq \sum_{i=1}^{k} \lambda^{k-i}[\hat{z}^{\mathrm{T}}(i)R_z\hat{z}(i) + (\Phi_{\mathrm{f}}(i)\hat{\theta})^{\mathrm{T}}R_{\mathrm{f}}\Phi_{\mathrm{f}}(i)\hat{\theta}] + \lambda^k(\hat{\theta} - \theta(0))^{\mathrm{T}}R_\theta(\hat{\theta} - \theta(0)), \tag{23}$$

where $R_z \in \mathbb{R}^{l_z}$ and $R_\theta \in \mathbb{R}^{l_z}$ are positive definite, $R_{\mathrm{f}} \in \mathbb{R}^{l_u}$ is positive semidefinite, and $\lambda \in (0, 1]$ is the forgetting factor. The following result is based on standard RLS theory [36].

PROPOSITION 1 Let $P(0) = R_\theta^{-1}$. Then, for all $k \geq 1$, the retrospective cost function (23) has the unique global minimizer $\theta(k)$ given by the RLS update

$$\theta(k) = \theta(k-1) - P(k-1)\Phi_{\mathrm{f}}^{\mathrm{T}}(k)\Gamma^{-1}(k)[\Phi_{\mathrm{f}}(k)\theta(k-1) + (R_z + R_{\mathrm{f}})^{-1}R_z(z_{\mathrm{f}}(k) - u_{\mathrm{f}}(k))], \tag{24}$$

where

$$P(k) = \frac{1}{\lambda}P(k-1) - \frac{1}{\lambda}P(k-1)\Phi_{\mathrm{f}}^{\mathrm{T}}(k)\Gamma^{-1}(k)\Phi_{\mathrm{f}}(k)P(k-1) \tag{25}$$

and

$$\Gamma(k) \triangleq \lambda(R_z + R_{\mathrm{f}})^{-1} + \Phi_{\mathrm{f}}(k)P(k-1)\Phi_{\mathrm{f}}^{\mathrm{T}}(k). \tag{26}$$

IV. MANEUVERING TARGET TRACKING

A. Maneuvering Target Tracking Model

Consider the discrete-time maneuvering planar target kinematics model

$$x(k) = Ax(k-1) + Bu(k-1) + w(k-1), \tag{27}$$

$$y(k) = Cx(k) + v(k), \tag{28}$$

where $x(k) \in \mathbb{R}^4$ is the state, $u(k) \in \mathbb{R}^2$ is the input acceleration, $w(k) \in \mathbb{R}^4$ is the process noise signal with positive-semidefinite covariance $Q(k) \in \mathbb{R}^{4\times4}$, $y(k) \in \mathbb{R}^2$ is the position measurement, and $v(k) \in \mathbb{R}^2$ is the measurement noise signal with positive-semidefinite covariance $R(k) \in \mathbb{R}^{2\times2}$. In (27), the state vector $x(k)$ is

$$x(k) = \begin{bmatrix} x_1(k) & x_2(k) & x_3(k) & x_4(k) \end{bmatrix}^{\mathrm{T}}, \tag{29}$$

where $x_1(k)$ and $x_3(k)$ are the planar coordinates of the maneuvering target; $x_2(k)$ and $x_4(k)$ are the velocity components of the maneuvering target; the input vector

$u(k)$ is

$$u(k) = \left[u_1(k)\ u_2(k)\right]^{\mathrm{T}}, \tag{30}$$

where $u_1(k)$ and $u_2(k)$ are the acceleration components of the maneuvering target; and

$$A \triangleq \begin{bmatrix} 1 & T & 0 & 0 \\ 0 & 1 & 0 & 0 \\ 0 & 0 & 1 & T \\ 0 & 0 & 0 & 1 \end{bmatrix}, B \triangleq \begin{bmatrix} T^2/2 & 0 \\ T & 0 \\ 0 & T^2/2 \\ 0 & T \end{bmatrix}, C \triangleq \begin{bmatrix} 1 & 0 \\ 0 & 0 \\ 0 & 1 \\ 0 & 0 \end{bmatrix}^{\mathrm{T}}, \tag{31}$$

where T is the sample time.

B. Simulation Example

Based on (1) and (2), we use KF/RCIE to track a simulated maneuvering target and compare the performance with the CA model–based Kalman filter (CAKF) [1], IMM estimator [11], and window-based least squares estimator (WLSE) [16]. Both the CA model and the CAKF filter are sixth order, and both consider the input acceleration as a component of the augmented state vector. Suppose that the initial position and velocity of the maneuvering target are $x(0) = [-100\ \text{m}, 10\ \text{m/s}, -30\ \text{m}, 5\ \text{m/s}]^{\mathrm{T}}$. For all estimators, we set the initial state estimates to be zero and start the estimators at $k = 25$. In accordance with (31), position measurement $x_1(k)$ and $x_3(k)$ are assumed to be available. The position of the target is sampled with $T = 1$ s, and the covariance of the measurement noise $v(k)$ is $R(k) = 100I_2$.

We test 50 sets of maneuvering target data with random measurement noise. The acceleration inputs in the x direction and y direction are

$$u_1(k) = \begin{cases} 0 & k < 300, \\ (0.01k - 3)^2 & 800 \geq k \geq 300, \\ 24 & 1300 \geq k > 800, \\ 24 - (0.01k - 13)^2 & 1700 \geq k > 1300, \\ 0 & k > 1700. \end{cases} \tag{32}$$

$$u_2(k) = \begin{cases} 0 & k < 300, \\ (15 - 0.05k)\sin(0.004k + 1.2) & 1700 \geq k \geq 300, \\ 0 & k > 1700. \end{cases} \tag{33}$$

For RCIE, let $G_{\mathrm{f}_u}(\mathbf{z}) \triangleq \sum_{i=0}^{8} H_i \mathbf{z}^{-i}$, where $H_i \triangleq CA^{i-1}B$ is the ith Markov parameter, the estimator order is $n_e = 8$, the performance weighting is $R_z = 0.5$, the input weighting is $R_{\mathrm{f}} = 1$, the parameter weighting is $R_\theta = 0.1$, and the forgetting factor is $\lambda = 1$. For the Kalman filter, the forecast error covariance is $P_{\mathrm{f}}(0) = 10I_4$, and the process noise covariance is $Q(k) = I_4$. For CAKF, the forecast error covariance is $P_{\mathrm{CA}}(0) = 10I_6$, and the process noise covariance is $Q_{\mathrm{CA}}(k) = I_6$. For WLSE, the tracking window size is $s_w = 5$, the forecast error covariance is $P_{\mathrm{WLSE}}(0) = 10I_4$, and the process noise covariance is $Q_{\mathrm{WLSE}}(k) = I_4$. For the IMM estimator, the constant velocity (CV) model and CA model are used. The process covariance of the CV model and CA model in the IMM estimator are the same as $Q(k)$ and $Q_{\mathrm{CA}}(k)$, respectively; the forecast error covariance of the CV model and CA model in the IMM estimator are the same as $P_{\mathrm{f}}(0)$ and $P_{\mathrm{CA}}(0)$, respectively; the initial model probability of the CV model and CA model are $\mu_{\mathrm{CV}} = 0.5$ and $\mu_{\mathrm{CA}} = 0.5$, respectively; and the mode transition probability is

$$\Pi = \begin{bmatrix} 0.97 & 0.03 \\ 0.03 & 0.97 \end{bmatrix}.$$

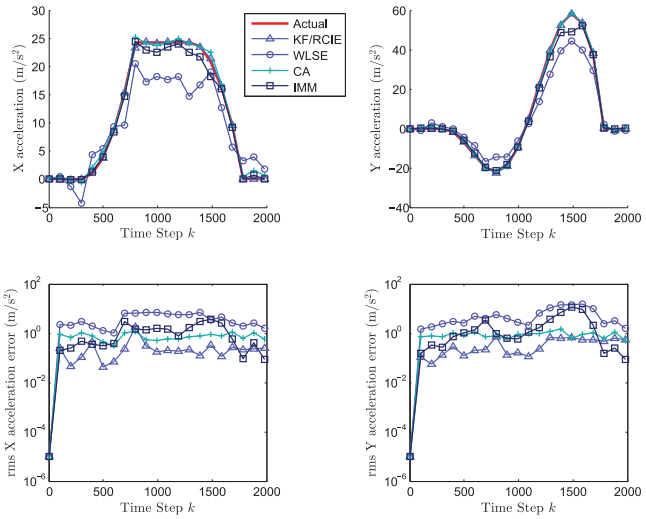

(a) Actual input, estimated input, and input RMS error

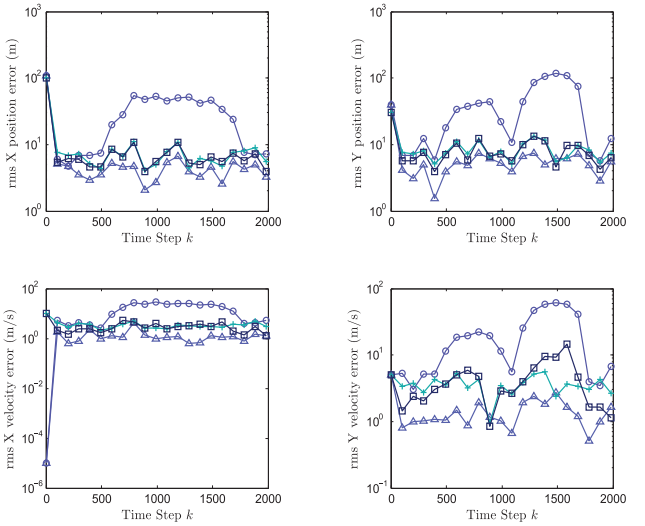

(b) State RMS error

Fig. 2. Actual input, estimated input, and RMS error of the state and input estimates. The error plots show RMS values averaged over 50 simulation runs using the KF/RCIE, WLSE, CAKF, and IMM estimators. Estimation begins at $k = 25$. The RMS errors of the KF/RCIE state and input estimates are lower than those of the other estimators.

Fig. 2(a) shows the actual input, the estimated input, and the root-mean-square (RMS) error of the input. Note that the unknown acceleration is considered a separate input vector in KF/RCIE and WLSE. However, in CAKF and IMM, the unknown acceleration is considered as a component of the augmented state vector. Fig. 2(b) shows the RMS errors of the state estimate. The error plots show

Fig. 3. Rate table with target. The rate table provides a specified angular velocity. The target consists of two Optitrack markers placed on the circumference of the rate table.

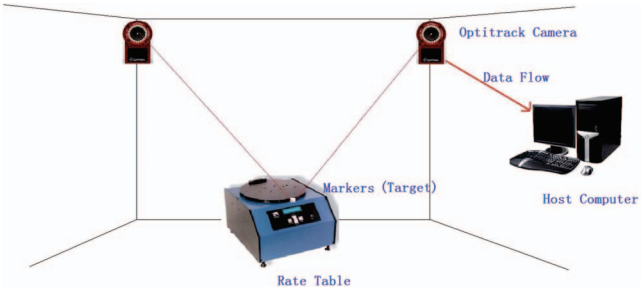

Fig. 4. Tracking system. The tracking system includes two Optitrack cameras, a target, a rate table, and a host computer. The Optitrack cameras measure the position of the target and transfer the data to the host computer.

the RMS values averaged over 50 simulation runs. It can be seen from Fig. 2a that KF/RCIE has the best input estimation performance among these estimators. In Figs. 2a and 2b, KF/RCIE produces the least RMS values of position, velocity, and acceleration.

V. RATE TABLE EXPERIMENT

The tracking system consists of an Optitrack camera system, Optitrack markers, a host computer, and a rate table. The Optitrack camera system, which includes several cameras, provides real-time position and orientation of a rigid body with two attached Optitrack markers. A target consists of two markers; the average position between the markers (Fig. 3) provides the target position. The Optitrack software uses reflected light to determine the position and orientation of the target. The rate table is normally used for testing and calibrating gyroscopic instruments.

A. Experimental Setup

The tracking system is shown in Fig. 4. Two cameras are placed so that the target motion can be observed by the Optitrack system. We calibrate the system and set the ground plane prior to the experiment using the Optitrack

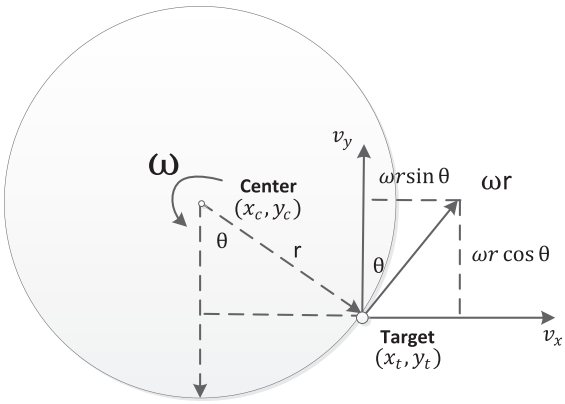

Fig. 5. Transformed reference frame. Using the position of the target, the radius of the rate table, and the angular velocity of the rate table. The rate table reference frame is transformed to the Optitrack system reference frame.

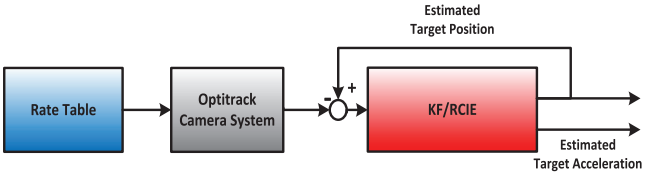

Fig. 6. Real-time Simulink model. This model includes the rate table block, Optitrack camera system block, and KF/RCIE estimator block. The input of the estimator is the position error.

calibration tools. Two Optitrack markers are placed on the circumference of the rate table, and the distance from the center to the circumference is the radius $r = 14.98$ cm. The camera system offers position information from the markers to the host computer.

By transforming the rate table reference frame to the Optitrack reference frame (Fig. 5), the velocity and acceleration in the latter frame have the form

$$x_2(k) = \omega r \sin(\omega k T), \tag{34}$$

$$x_4(k) = \omega r \cos(\omega k T), \tag{35}$$

$$a_x(k) = -\omega^2 r \sin(\omega k T), \tag{36}$$

$$a_y(k) = \omega^2 r \cos(\omega k T), \tag{37}$$

where $x_2(k)$ and $x_4(k)$ are the velocity components in the x and y directions, respectively; $a_x(k)$ and $a_y(k)$ are the acceleration components in the x and y directions, respectively; ω is the angular velocity of the rate table; T is the sample time; and r is the radius of the rate table.

This experiment is carried out using the real-time Simulink environment. We integrate the Optitrack camera system, KF/RCIE, and data storage as individual blocks, respectively. The real-time Simulink model structure is shown in Fig. 6.

B. Tracking System Example

EXAMPLE 5.1 In this experiment, the target starts at [0.29 m, 0.26 m]$^{\mathrm{T}}$. For all estimators, we set the initial state estimates to be zero. The position of the target is sampled with $T = 0.1$ s. The angular velocity is $\omega = 200°/\mathrm{s}$. Since the positions of the center of the circle and the target are available and r, ω, and T are known, (34)–(37) are used to compute the velocity and acceleration in the x and y directions, respectively. Since the acceleration of the target on the rate table is not zero, a nonmaneuvering target tracking model (e.g., CV model) will perform poorly in providing the state and input estimates. In the following experiments, we compare KF/RCIE with CAKF and WLSE.

For RCIE, let $G_{\mathrm{f}_u}(\mathbf{z}) \triangleq \sum_{i=0}^{12} H_i \mathbf{z}^{-i}$, where $H_i \triangleq CA^{i-1}B$ is the ith Markov parameter, the estimator order is $n_e = 12$, the performance weighting is $R_z = 0.01$, the input weighting is $R_{\mathrm{f}} = 10^{-10}$, the parameter weighting is $R_\theta = 0.1$, and the forgetting factor is $\lambda = 1$. For the Kalman filter, the forecast error covariance is $P_{\mathrm{f}}(0) = 10I_4$, the process noise covariance is $Q(k) = 0.001I_4$, and the measurement noise covariance is $R(k) = 10^{-8}I_2$. For CAKF, the forecast error covariance is $P_{\mathrm{CA}}(0) = 10I_6$, the process noise covariance is $Q_{\mathrm{CA}}(k) = 0.001I_6$, and the measurement noise covariance is $R_{\mathrm{CA}}(k) = 10^{-8}I_2$. For WLSE, the tracking window size is $s_w = 5$, the forecast error covariance is $P_{\mathrm{WLSE}}(0) = 10I_4$, the process noise covariance is $Q_{\mathrm{WLSE}}(k) = 0.001I_4$, and the measurement noise covariance is $R_{\mathrm{WLSE}}(k) = 10^{-8}I_2$.

Figs. 7(a) and 7(b) show the actual input and state as well as the RMS error of KF/RCIE, WLSE, and CAKF. The error plots show the RMS values averaged over 10 experimental tests. At the beginning, the RMS errors of the KF/RCIE state estimate are approximately equivalent to those of the other estimators. After a few steps, however, the RMS errors of the KF/RCIE state and input estimates decrease to approximately one order of magnitude lower than those of WLSE. The RMS errors of the KF/RCIE state and input estimates become lower than those of CAKF by 5%.

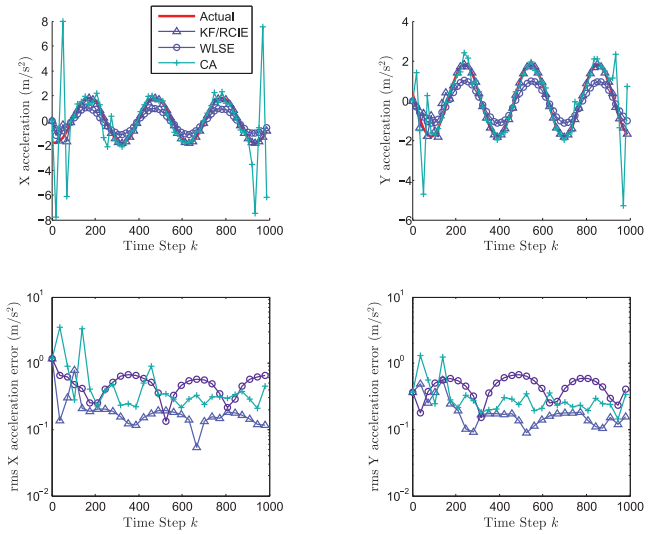

(a) Actual input, estimated input, and input RMS error

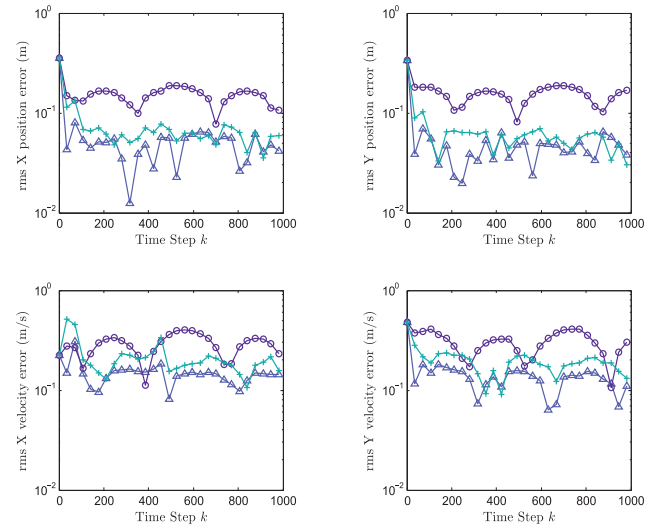

(b) State RMS error

Fig. 7. Actual input, estimated input, and RMS error of the state and input estimates for the tracking system with angular velocity $\omega = 200°/\mathrm{s}$. The error plots show RMS values averaged over 10 experimental tests using KF/RCIE, WLSE, and CAKF. Estimation begins at $k = 15$. At the beginning, the RMS errors of the KF/RCIE state estimate and those of CAKF and WLSE are approximately the same. After a few steps, however, the RMS errors of the KF/RCIE state and input estimates are approximately one order of magnitude lower than those of WLSE. Overall, KF/RCIE has the best performance among these estimators.

EXAMPLE 5.2 In this experiment, we degrade the accuracy of the position measurement by adding zero-mean white noise with covariance $R(k) = 0.0011I_2$ to the position measurement. The resulting signal-to-noise ratio (SNR) is 10. The target starts at [0.29 m, 0.26 m]$^{\mathrm{T}}$. For all estimators, we set the initial state estimates to be zero. The position of the target is sampled with $T = 0.1$ s. The angular velocity is $\omega = 200°/\mathrm{s}$. Since the actual state and input without additional white noise is available, we can compare estimates with the actual values.

For RCIE, let $G_{\mathrm{f}_u}(\mathbf{z}) \triangleq \sum_{i=0}^{12} H_i \mathbf{z}^{-i}$, where $H_i \triangleq CA^{i-1}B$ is the ith Markov parameter, the estimator order is $n_e =$ 12, the performance weighting is $R_z = 0.01$, the input weighting is $R_{\mathrm{f}} = 10^{-10}$, the parameter weighting is $R_\theta = 0.1$, and the forgetting factor is $\lambda = 1$. For the Kalman filter, the forecast error covariance is $P_{\mathrm{f}}(0) = 10I_4$, the process noise covariance is $Q(k) = 10^{-5}I_4$, and the measurement noise covariance is $R(k) = 0.0011I_2$. For CAKF, the forecast error covariance is $P_{\mathrm{CA}}(0) = 10I_6$, the process noise covariance is $Q_{\mathrm{CA}}(k) = 10^{-5}I_6$, and the measurement noise covariance is $R_{\mathrm{CA}}(k) = 0.001I_2$. For WLSE, the tracking window size is $s_w = 5$, the forecast error covariance is $P_{\mathrm{WLSE}}(0) = 10I_4$, the process noise

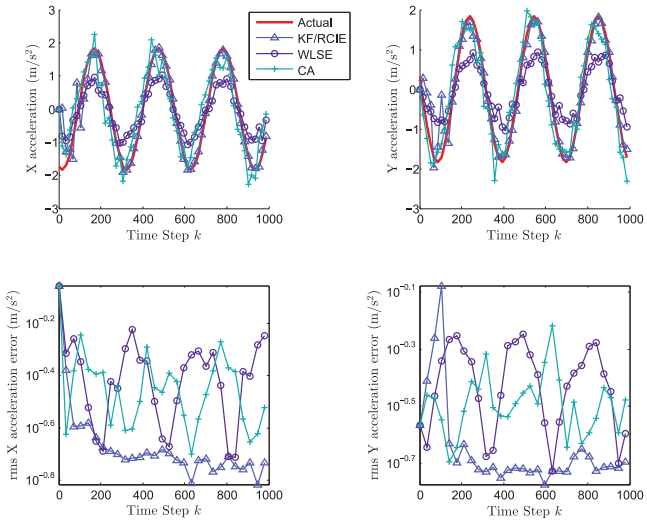

(a) Actual input, estimated input, and input RMS error

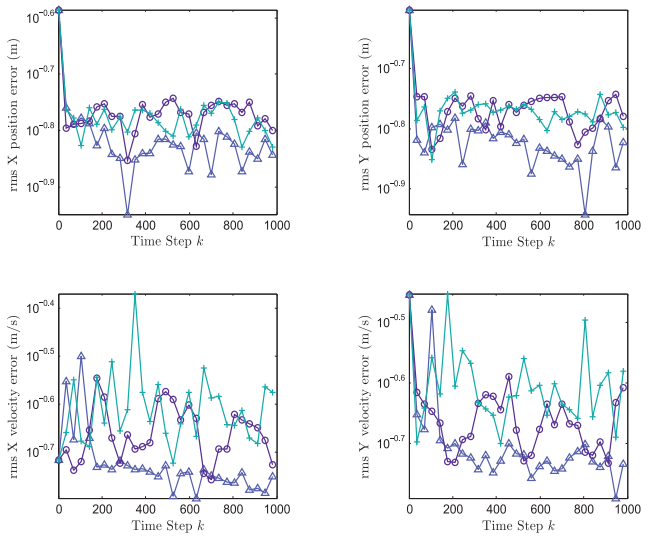

(b) State RMS error

Fig. 8. Actual input, estimated input, and RMS error of the state and input estimates for the tracking system with white measurement noise with SNR = 10. The error plots show RMS values averaged over 10 experimental tests using KF/RCIE, WLSE, and CAKF. Estimation begins at $k = 15$. In the presence of white measurement noise, the RMS errors of the KF/RCIE state estimate are slightly larger than those of the other estimators at the beginning. After a few steps, however, the RMS errors of the KF/RCIE state and input estimates are lower than those of CAKF and WLSE.

covariance is $Q_{\mathrm{WLSE}}(k) = 10^{-5} I_4$, and the measurement noise covariance is $R_{\mathrm{WLSE}}(k) = 0.0011 I_2$.

Figs. 8(a) and 8(b) display the actual input, the estimated input, and the RMS error of KF/RCIE, WLSE, and CAKF. The error plots show the RMS values averaged over 10 runs. At the beginning, the RMS errors of the KF/RCIE state estimate are slightly higher than those of the other estimators. After a few steps, however, the RMS errors of the KF/RCIE state and input estimates become lower than those of CAKF and WLSE by 5% and 15%, respectively.

VI. CONCLUSIONS

We considered maneuvering target tracking with unknown acceleration, and we formulated the KF/RCIE. We used KF/RCIE to track a maneuvering target with unknown acceleration, and we compared KF/RCIE with CAKF, WLSE, and IMM in simulation. We then applied KF/RCIE to maneuvering target tracking with measurement noise. Simulation results showed that KF/RCIE yielded more accurate state and acceleration estimates than CAKF, WLSE, and IMM.

For experimentation, we used a tracking system consisting of a rate table and Optitrack camera system. We installed the target on the circumference of the rate table and obtained the true velocity and acceleration by transforming the rate table frame to the Optitrack camera system frame. We then used KF/RCIE with the camera data to estimate the target acceleration along with the target position and velocity. Compared with CAKF and WLSE, KF/RCIE provided more accurate state estimates in the presence of noise added to the data.

REFERENCES

[1] Li, X. R., and Jilkov, V. P.
Survey of maneuvering target tracking. Part I. Dynamic models.
IEEE Transactions on Aerospace and Electronic Systems, **39**, 4 (Oct. 2003), 1333–1364.

[2] Yuan, X., Han, C., Duan, Z., and Lei, M.
Adaptive turn rate estimation using range rate measurements.
IEEE Transactions on Aerospace and Electronic Systems, **42**, 4 (Oct. 2006), 1532–1541.

[3] Singer, R. A.
Estimating optimal tracking filter performance for manned maneuvering targets.
IEEE Transactions on Aerospace and Electronic Systems, **AES-6**, 4 (Jul. 1970), 473–483.

[4] Singer, R. A., and Behnke, K. W.
Real-time tracking filter evaluation and selection for tactical applications.
IEEE Transactions on Aerospace and Electronic Systems, **AES-7**, 1 (Jan. 1971), 100–110.

[5] Ng, W., Ji, C., Ma, W-K., and So, H. C.
A study on particle filters for single-tone frequency tracking.
IEEE Transactions on Aerospace and Electronic Systems, **45**, 3 (Jul. 2009), 1111–1125.

[6] Zhou, H., and Kumar, K.
A "current" statistical model and adaptive algorithm for estimating maneuvering targets.
Journal of Guidance, Control, and Dynamics, **7**, 5 (Oct. 1984), 596–602.

[7] Mahapatra, P. R., and Mehrotra, K.
Mixed coordinate tracking of generalized maneuvering targets using acceleration and jerk models.
IEEE Transactions on Aerospace and Electronic Systems, **36**, 3 (Jul. 2000), 992–1000.

[8] Ghosh, S., and Mukhopadhyay, S.
Tracking reentry ballistic targets using acceleration and jerk models.
IEEE Transactions on Aerospace and Electronic Systems, **47**, 1 (Jan. 2011), 666–683.

[9] Kirubarajan, T., Bar-Shalom, Y., Pattipati, K. R., and Kadar, I.
Ground target tracking with variable structure IMM estimator.
IEEE Transactions on Aerospace and Electronic Systems, **36**, 1 (Jan. 2000), 26–46.

[10] Johnston, L. A., and Krishnamurthy, V.
An improvement to the interacting multiple model (IMM) algorithm.
IEEE Transactions on Signal Processing, **49**, 12 (Dec. 2001), 2909–2923.

[11] Seah, C. E., and Hwang, I.
Algorithm for performance analysis of the IMM algorithm.
IEEE Transactions on Aerospace and Electronic Systems, **47**, 2 (Apr. 2011), 1114–1124.

[12] Nadarajah, N., Tharmarasa, R., McDonald, M., and Kirubarajan, T.
IMM forward filtering and backward smoothing for maneuvering target tracking.
IEEE Transactions on Aerospace and Electronic Systems, **48**, 3 (Jul. 2012), 2673–2678.

[13] Yuan, T., Bar-Shalom, Y., Willett, P., Mozeson, E., Pollak, S., and Hardiman, D.
A multiple IMM estimation approach with unbiased mixing for thrusting projectiles.
IEEE Transactions on Aerospace and Electronic Systems, **48**, 4 (Oct. 2012), 3250–3267.

[14] Mazor, E., Averbuch, A., Bar-Shalom, Y., and Dayan, J.
Interacting multiple model methods in target tracking: a survey.
IEEE Transactions on Aerospace and Electronic Systems, **34**, 1 (Jan. 1998), 103–123.

[15] Wang, X., Challa, S., Evans, R., and Li, X. R.
Minimal submodel-set algorithm for maneuvering target tracking.
IEEE Transactions on Aerospace and Electronic Systems, **39**, 4 (Oct. 2003), 1218–1231.

[16] Chan, Y., Hu, A., and Plant, J.
A Kalman filter based tracking scheme with input estimation.
IEEE Transactions on Aerospace and Electronic Systems, **AES-15**, 2 (Mar. 1979), 237–244.

[17] Bogler, P.
Tracking a maneuvering target using input estimation.
IEEE Transactions on Aerospace and Electronic Systems, **AES-25**, 2 (Mar. 1989), 298–310.

[18] Lee, H.
Generalized input-estimation technique for tracking maneuvering targets.
IEEE Transactions on Aerospace and Electronic Systems, **35**, 4 (Oct. 1999), 1388–1402.

[19] Khaloozadeh, H., and Karsaz, A.
Modified input estimation technique for tracking manoeuvring targets.
IET Radar, Sonar & Navigation, **3**, 1 (2009), 30–41.

[20] Kitanidis, P. K.
Unbiased minimum-variance linear state estimation.
Automatica, **23**, 6 (1987), 775–778.

[21] Gillijns, S., and Moor, B. D.
Unbiased minimum-variance input and state estimation for linear discrete-time systems.
Automatica, **43**, 1 (Jan. 2007), 111–116.

[22] Floquet, T., and Barbot, J. P.
State and unknown input estimation for linear discrete-time systems.
Automatica, **42**, 11 (Nov. 2006), 1883–1889.

[23] Sundaram, S., and Hadjicostis, C. N.
Delayed observers for linear systems with unknown inputs.
IEEE Transactions on Automatic Control, **52**, 2 (Feb. 2007), 334–339.

[24] Xiong, Y., and Saif, M.
Unknown disturbance inputs estimation based on a state functional observer design.
Automatica, **39**, 8 (Aug. 2003), 1389–1398.

[25] Santillo, M. A., and Bernstein, D. S.
Adaptive control based on retrospective cost optimization.
Journal of Guidance, Control, and Dynamics, **33**, 2 (Mar. 2010), 289–304.

[26] Hoagg, J. B., and Bernstein, D. S.
Retrospective cost model reference adaptive control for nonminimum-phase systems.
Journal of Guidance, Control, and Dynamics, **35**, 6 (Nov. 2012), 1767–1786.

[27] Ali, A. A., Goel, A., Ridley, A. J., and Bernstein, D. S.
Retrospective-cost-based adaptive input and state estimation for the ionosphere-thermosphere.
Journal of Aerospace Information Systems, **12**, 12 (Dec. 2015), 767–783. DOI:10.2514/1.I010286.

[28] D'Amato, A. M., Springmann, J., Ali, A. A., Cutler, J., Ridley, A., and Bernstein, D. S.
Adaptive state estimation for nonminimum-phase systems with uncertain harmonic inputs.
In *Proceedings of AIAA Guidance, Navigation and Control Conference*, Portland, OR, Aug. 2011, 1885–1902.

[29] Gupta, R., D'Amato, A. M., Ali, A. A., and Bernstein, D. S.
Retrospective-cost-based adaptive state estimation and input reconstruction for a maneuvering aircraft with unknown acceleration.
In *Proceedings of AIAA Guidance, Navigation and Control Conference*, Minneapolis, MN, Aug. 2012, 1536–1555.

[30] Lee, B., Park, J., Joo, Y., and Jin, S.
Intelligent Kalman filter for tracking a manoeuvring target.
IEE Proceedings Radar, Sonar and Navigation, **151**, 6 (Dec. 2004), 344–350.

[31] Ru, J., Jilkov, V. P., Li, X. R., and Bashi, A.
Detection of target maneuver onset.
IEEE Transactions on Aerospace and Electronic Systems, **45**, 2 (Apr. 2009), 536–554.

[32] Lan, J., and Li, X. R.
Equivalent-model augmentation for variable-structure multiple-model estimation.
IEEE Transactions on Aerospace and Electronic Systems, **49**, 4 (Oct. 2013), 2615–2630.

[33] Lin, C., and Hsueh, C.
Adaptive EKF-CMAC-based multisensor data fusion for maneuvering target.
IEEE Transactions on Instrumentation and Measurement, **62**, 7 (Jul. 2013), 2058–2066.

[34] Horst, J., Oispuu, M., and Koch, W.
Accuracy study for a piecewise maneuvering target with unknown maneuver change times.
IEEE Transactions on Aerospace and Electronic Systems, **50**, 1 (Jan. 2014), 737–755.

[35] Li, Y., Li, X., and Wang, H.
Target tracking in a collaborative sensor network.
IEEE Transactions on Aerospace and Electronic Systems, **50**, 4 (Oct. 2014), 2694–2714.

[36] Astrom, K. J., and Wittenmark, B. *Adaptive Control* (2nd ed.).
Boston: Addison-Wesley, 1995.

Liang Han received his B.E. degree in automation from Nanjing University of Science and Technology, Nanjing, China, in 2011. He has been a research scholar in the Aerospace Engineering Department, University of Michigan, Ann Arbor, from 2013 to 2014. He is now a doctoral student in the School of Automation Science and Electrical Engineering, Beihang University, Beijing, China. His research interests include target tracking and cooperative control of multiagent systems.

Zhang Ren received his B.E., M.E., and Ph.D. degrees in aircraft guidance, navigation, and simulation from Northwestern Polytechnical University, Xi'an, China, in 1982, 1985, and 1994, respectively. From 1995 to 1998, he was a professor in the School of Marine Engineering, Northwestern Polytechnical University, Xi'an, China. From 1999 to 2000, he held the visiting professor positions with University of California, Riverside, and Louisiana State University, Baton Rouge, respectively. He is now a professor with the School of Automation Science and Electrical Engineering, Beihang University, Beijing, China, and also the recipient of the Chang Jiang Professorship awarded by the Education Ministry of China. His research interests include aircraft guidance, navigation and control, fault detection, isolation and recovery, and cooperative control of multiagent systems.

Dennis S. Bernstein received his Sc.B. degree in applied mathematics from Brown University, Providence, Rhode Island, in 1977 and his Ph.D. degree in control engineering from the University of Michigan, Ann Arbor, in 1982, where he is currently professor in the Aerospace Engineering Department. His interests are in estimation and control for aerospace applications. He is the author of *Matrix Mathematics* published by Princeton University Press.